Inorg. Chem. **2008**, *47*, 8233−8241

Hydration Properties of Aqueous Pb(II) Ion

Matthew C. F. Wander and Aurora E. Clark*

Department of Chemistry, Washington State University, Pullman, Washington 99164

Received April 25, 2008

Using density functional theory and polarized continuum models, we have determined the most probable coordination number and structure of the first hydration shell of aqueous Pb(II). The geometries and hydration free energies of $Pb(H_2O)_{1-9}^{2+}$ were examined and benchmarked against experimental values. The free energies of hydration of $Pb(H_2O)_{6-8}^{2+}$ were found to match the experimental value within 10 kcal/mol. Moreover, based upon our thermochemical results for single water addition, primary hydration numbers of 6, 7, and 8 are all thermally accessible at STP. Use of a small-core 60 electron effective core potential (ECP) with the aug-cc-pvdz-PP basis on Pb resulted in structures that are significantly less hemidirected than predicted when using the large-core 78 electron ECP and the lanl2DZ basis on the metal. Our results imply that the hemi- to holo-directed transition in Pb(II)-water complexes is driven by coordination number and not hybridization of the 6*s* lone-pair orbital or enhanced covalent bonding in the $Pb-OH_2$ bond. In addition to basis set effects, the influence of different solvation models on hydration reactions has further been examined so as to determine the relative accuracy of the calculated hydration thermochemistry.

Introduction

As a toxin the behavior of Pb has been long understood; however, much less effort has been devoted to understanding its fundamental aqueous chemistry. Despite the elimination of lead from gasoline, its continued use in other industrial applications (e.g., electronics, batteries, glass, and projectiles) causes continued environmental relevance of the solution phase behavior of Pb. Despite this importance, very little experimental evidence exists to quantify its aqueous properties. Under normal environmental conditions, Pb is in the (II) oxidation state (the $[Xe]4f^{14}5d^{10}6s^26p^0$ electronic configuration), though in certain environments it can be found in the (IV) oxidation state, (e.g., organo-lead compounds such as the gasoline additive tetraethyllead).[1] Basic thermodynamic parameters of hydration have been derived by Marcus for the (II) oxidation state: $\Delta G_{hyd}(Pb^{2+}) = -6$ kcal/mol, $\Delta H_{hyd}(Pb^{2+}) = -375.7$ kcal/mol, $\Delta V_{hyd} = -26.5$ cm^3/mol, Cp $= -50.0$ cal/mol K, based upon the NBS tables of chemical thermodynamic properties.[2−9] The water exchange rate between the primary and secondary hydration shells has also been experimentally measured at 1×10^9 s^{-1}.[10] In spite of the available thermodynamic and kinetic data, only limited solution phase spectroscopic evidence (NMR) has identified the specific coordination number as ∼5.7.[11] Solid-state X-ray and surface extended X-ray absorption fine structure (EXAFS) data regarding the hydration of Pb^{2+} is limited; however, complexes that span holo-directed structures in ionic and hemi-directed structures in covalent Pb(II) complexes have been reported.[12] Figure 1a shows a diagrammatic representation of the uniform ligand distribution associated with holo-directed structures, while in Figure 1b the Pb lone pair presumably directs the ligands to preferentially bind on one side of the molecule (hemi-directed). In the latter, a variety of calculations on Pb(II) complexes in the gas-phase using second order Moller−Plessett perturbation theory

* To whom correspondence should be addressed. E-mail: auclark@wsu.edu.

(1) Claudio, E. S.; Godwin, H. A.; Magyar, J. S. *Prog. Inorg. Chem.* **2003**, *51*, 1–144.
(2) Marcus, Y. *Pure Appl. Chem.* **1987**, *59* (9), 1093–1101.
(3) Marcus, Y. *J. Chem. Soc., Faraday Trans. I* **1987**, *83*, 339–349.
(4) Abraham, M. H.; Marcus, Y. *J. Chem. Soc., Faraday Trans. I* **1986**, *82*, 3255–3274.
(5) Marcus, Y. *J. Chem. Soc., Faraday Trans.* **1991**, *87* (18), 2995–2999.
(6) Abraham, M. H.; Marcus, Y.; Lawrence, K. G. *J. Chem. Soc., Faraday Trans. I* **1988**, *84*, 175–185.
(7) Marcus, Y. *J. Solution Chem.* **1994**, *23* (7), 831–848.
(8) Marcus, Y. *Biophys. Chem.* **1994**, *51* (2−3), 111–127.
(9) Marcus, Y. *J. Chem. Soc., Faraday Trans.* **1993**, *89* (4), 713–718.
(10) Stumm, W.; Morgan, J. J. *Aquatic chemistry: Chemical equilibria and rates in natural waters*, 3rd ed.; Wiley-Interscience: New York, 1995; p 1022.
(11) Marcus, Y. *Ion Solvation*; John Wiley and Sons Ltd: New York, 1985; p 77.
(12) Bargar, J. R.; Brown, G. E.; Parks, G. A. *Geochim. Cosmochim. Acta* **1997**, *61* (13), 2617–2637.

10.1021/ic800750g CCC: $40.75
Published on Web 08/21/2008

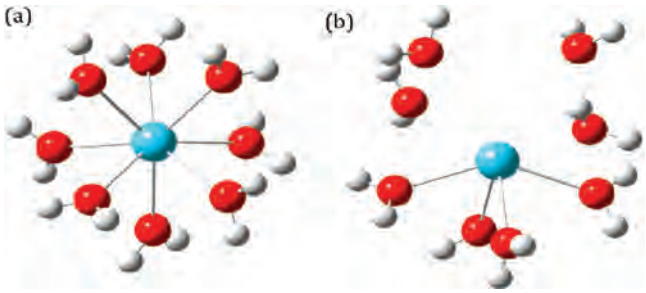

Figure 1. (a) Holo- and (b) hemidirected ligand binding to Pb^{2+}.

(MP2) and density functional theory (DFT) with the lanl2DZ+d basis indicate that the Pb lone-pair is primarily 6s in nature but is polarized by the inclusion of p-AO character.[13,14] Other factors that affect the presence of hemi- vs holo-directed bonding include repulsive interactions among ligands, high charge transfer, ionic bonding, and ligand-ligand repulsions. On the basis of the prior calculations, it has been concluded that holo-directed structures require both high coordination numbers and strongly electron donating (soft) ligands, which increases the p-character in the Pb-X bond and makes it more covalent. In contrast, hemi-directed structures are observed primarily in complexes formed from weakly electron-donating (hard) ligands under low coordination numbers, wherein there is p-character in the lone-pair orbital rather than the Pb-X bonding orbitals (subsequently leading to more ionic Pb-X bonding).[14]

Similar to the gas-phase theoretical studies, examples of DFT (B3LYP functional) calculations of organo-aqueous Pb(II) complexes have utilized the relatively modest lanl2DZ relativistic effective core potential (RECP) and its associated basis to describe the electronic structure of the Pb^{2+} ions. This replaces 78 core electrons and describes the remaining $6s^2$ valence electrons by a contracted [2s 2p] basis set. Further, these studies have frequently neglected the role of water, omitting explicit waters within the solvation shell. The result has been almost exclusively hemi-directed structures.[15−18] Combined quantum mechanical and classical molecular dynamics studies (QM/CMD) have investigated the aqueous hydration of Pb(II) using Hartree−Fock theory and the SBKJC VDZ basis and effective core potential (ECP) on Pb and the DZP basis on water within the inner hydration shell of Pb^{2+}, and a classical BJH-CF2 model for the remaining waters.[19,20] This study predicted a primary hydration coordination number (CN) of nine for Pb^{2+}, with a hydration free energy of −535 kcal/mol, nearly 200 kcal/mol different from experiment.[19,20] A second QM/CMD study using B3LYP and the 78 e- ECP and basis on the Pb^{2+} and the 6−31+G** basis on water predicted a hydration number of 7.[21] Thus, previous work on aqueous Pb(II) has predicted extreme deviations in the primary coordination sphere and hydration thermochemistry.

To accurately describe Pb-bonding both method and basis set must be used that have demonstrated success describing late transition metals and water solvation chemistry. To complicate matters, accurate descriptions of sterically active lone pairs (as is present in Pb(II)) are difficult to obtain and can have a significant influence upon the geometry.[22,23] In this study, we examine the structural, electronic, and thermodynamic aspects of unimolecular addition of water for Pb(II) from the mono- to nonaaqua species and calculate the free energy and enthalpy of hydration of species relevant to the solution phase. While coupled cluster methodologies would be ideal to accurately study the steric activity of the Pb(II) lone pair orbital, these are computationally impractical for Pb and thus density functional theory has been used. Particular attention has been paid to the structures from both the traditionally used lanl2DZ basis (using a 78 e- RECP) and the larger aug-cc-pvdz-PP basis (using a 60 e- RECP), and the importance of the inclusion of solvation effects using various polarized continuum models. These results are compared with the existing experimental values to determine the most likely structure(s) in aqueous solution. Further, we examine the role of water clusters in the accuracy of these calculations. On the basis of both sets of data, we have predicted both the static and potential dynamic hydration number for Pb(II).

Computational Methods

Hybrid DFT calculations were performed using Gaussian03[23] to elucidate the geometric and electronic structures of $Pb(H_2O)_{1-9}^{2+}$. Specifically, we used the B3LYP combination of exchange and correlation functionals with the aug-cc-pvdz-PP basis on Pb and the aug-cc-pvdz basis on H- and O-atoms.[24−28] This method and basis set has been shown to yield reasonable structures and energetic results for a variety of late transition metal and rare earth aqueous systems.[29−31] Initial optimizations used the 78 e- lanl2 RECP and lanl2DZ[32,33] basis on Pb (described by [2s, 2p] contracted gaussians), O, and H; however, this basis led to unstable $Pb(H_2O)_{5-9}^{2+}$ complexes, shown subsequently. The larger aug-cc-pvdz-PP basis

(13) Shimoni-Livny, L.; Glusker, J. P.; Bock, C. W. *Inorg. Chem.* **1998**, *37*, 1853–1867.
(14) Gourlaouen, C.; Gerard, H.; Piquemal, J.-P.; Parisel, O. *Chem.—Eur. J.* **2008**, *14*, 2730–2743.
(15) Breza, M.; Manova, A. *Polyhedron* **1999**, *18*, 2085–2090.
(16) Breza, M.; Biskupic, S.; Manova, A. *Polyhedron* **2003**, *22*, 2863–2867.
(17) Breza, M.; Manova, A. *J. Mol. Struct.* **2006**, *765*, 121–126.
(18) Bengtsson, L. A.; Hoffmann, R. *J. Am. Chem. Soc.* **1993**, *115*, 2666–2676.
(19) Hofer, T. S.; Randolf, B. R.; Rode, B. M. *J. Chem. Phys.* **2006**, *323*, 473–478.
(20) Hofer, T. S.; Rode, B. M. *J. Chem. Phys.* **2004**, *121*, 6406–6411.
(21) Gourlaouen, C.; Gerard, H.; Parisel, O. *Chem.—Eur. J.* **2006**, *12*, 5024–5032.
(22) Dixon, D. A.; Grant, D. J.; Christe, K. O.; Peterson, K. A. *Inorg. Chem.* **2008**, *48*, 5485–5494.
(23) Dixon, D. A.; de Jong, W. A.; Peterson, K. A.; Christe, K. O.; Schrobilgen, G. J. *J. Am. Chem. Soc.* **2005**, *127*, 8627–8624.
(24) Becke, A. D., III *J. Chem. Phys.* **1993**, *98*, 5648–5652.
(25) Stevens, P. J.; Devlin, F. J.; Chabalowski, C. F.; Frisch, M. J. *J. Phys. Chem.* **1994**, *98* (45), 11623–11627.
(26) Peterson, K. A.; Figgen, D.; Goll, E.; Stoll, H.; Dolg, M.; Harrison, R. J. *J. Chem. Phys.* **2003**, *119*, 11113.
(27) Dunning, T. H., Jr *J. Chem. Phys.* **1989**, *90*, 1007.
(28) Kendall, R. A.; Dunning, T. H., Jr *J. Chem. Phys.* **1992**, *96*, 6796.
(29) Dinescu, A.; Clark, A. E. *J. Phys. Chem. A*, submitted for publication.
(30) Chen, D. L.; Tian, W. Q.; Feng, J. K.; Sun, C. C. *J. Phys. Chem. A* **2007**, *111* (33), 8277–8280.
(31) Chen, D. L.; Tian, W. Q.; Sun, C. C. *Physical Review A* **2007**, *75* (1), 013201.
(32) Check, C. E.; Faust, T. O.; Bailey, J. M.; White, B. J.; Gilbert, T. M.; Sunderlin, L. S. *J. Phys. Chem. A* **2001**, *105*, 8111–8116.
(33) Ortiz, J. V.; Hay, P. J.; Martin, R. L. *J. Am. Chem. Soc.* **1992**, *114* (7), 2736–2737.

set for Pb uses a small core ECP, which replaces the inner 60 electrons (corresponding to the $1s^2 2s^2 2p^6 3s^2 3p^6 4s^2 3d^{10} 4p^6 4d^{10} 3f^{14}$ core electron configuration), leaving the $5s^2 5p^6 6s^2 5d^{10} 6p^2$ electrons in the valence (described by [5s, 4p, 3d] contracted gaussians) while incorporating relativistic corrections. Geometry optimizations used initial geometries based upon idealized structures from ligand field theory, and gas phase frequency calculations employed a tight SCF energy convergence of 10^{-8} and an ultrafine grid for numerical integration, as did the single point polarized continuum model (PCM) calculations. No symmetry constraints were imposed during the optimizations with the exception of the $Pb(H_2O)_9^{+2}$ structure where C_3 symmetry was imposed. Gas phase optimizations and frequency calculations are reported with solvent corrections obtained by single point calculations using the PCM.[34,35] The results utilizing UA0, UFF, and Pauling ($\alpha = 1.1$) PCM cavities were also compared. Natural bond order (NBO) and population analyses (NPA) were performed to analyze the electronic structure using a modified valence space containing the 6s6p5d4f Pb natural atomic orbitals (NAOs).[36,37] Hydration thermodynamics calculations utilized B3LYP optimized $(H_2O)_{1-9}$ water clusters using the aug-cc-pvdz basis.

Thermodynamic values for ΔG_{solv} and ΔH_{solv} were obtained using the PCM within the context of

$$\Delta G_{solv} = \sum G_{react} - \sum G_{prod} \tag{1}$$

The free energy of a species is expressed as

$$G = E^0_{gas} + G_{corr} + G_{scrf} + G_{SS} \tag{2}$$

where

$$G_{corr} = PV - TS \tag{2a}$$

and

$$E^0_{gas} = E_{gas} + E_{ZPE} + E_{thermal} \tag{2b}$$

and

$$G_{scrf} = G_{electrostatic} + G_{non\text{-}electrostatic} = G_{electrostatic} + G_{cavitation} + G_{dispersion} + G_{repulsion} \tag{2c}$$

and

$$G_{electrostatic} = E_{electrostatic} = E_{pcm} - E_{gas} \tag{2d}$$

In the case of water

$$G_{SS} = RT \ln(P_w/P^0)/n \tag{2e}$$

otherwise the term is 0. Starting with eq 2a, P is the pressure of the gas phase calculation, V is the volume, T is the temperature, and S is the entropy. In eq 2a, E_{gas} is the gas phase energy solution of the Hamiltonian, E_{ZPE} is the zero point correction, and $E_{thermal}$ is the thermal correction to the energy. In eqs 2c and 2d, the PCM free energy is decomposed into electrostatic and non-electrostatic components. The non-electrostatic components (cavitation, dispersion, and repulsion) correspond to the energy required to create the cavity, while the electrostatic component (the difference of the Hamiltonian energies of the system in solvent (E_{pcm}) and gas-phase (E_{gas})) is primarily dependent on the dielectric of the solvent. In eq 2e, we take into account that the pressure in the PCM is not the same as in the standard state. P_w is the pressure of liquid water assuming it is an ideal gas, P^0 is the pressure of the gas phase standard state, R is the universal gas constant, and T is the temperature in kelvin. Water is present in liquid at a concentration of 55.56 M or about 1350 atm. This corresponds to 4.3 kcal mol^{-1}/n, where n = number of water in the cluster.[38]

For enthalpy, the process is a little more complicated as explicit forms do not exist for the non-electrostatic contributions to the enthalpy. We need a return to more fundamental expressions of the basic thermodynamic relationships:

$$\left(\frac{\partial \Delta G}{\partial T}\right)_P = -\Delta S \tag{3}$$

and employing the Helmholtz equation

$$H = G - T\left(\frac{\partial G}{\partial T}\right)_P \tag{3a}$$

Then, the entropy is calculated numerically as

$$S(T) = \frac{G(T + \Delta T) - G(T - \Delta T)}{2\Delta T} \tag{3b}$$

where $\Delta T = 25$ °C. This value of ΔT was selected for this work because (1) it is large enough that computational errors are not larger than the energy differences of interest, (2) it is small enough that C_p is approximately constant over the entire temperature range, (3) water is still expected to be liquid in the temperature range, and (4) it is within the recommended range of values by Tomasi et al.[39] In Gaussian03 it is not possible to change the temperature of a PCM calculation, only the dielectric constant; thus, several PCM calculations were performed at different dielectrics corresponding to the dielectric of water within ΔT: $\varepsilon = 64.94$ at 323 K; $\varepsilon = 88.00$ at 273 K. Because the temperature could not be altered directly, the non-electrostatic terms remain constant. Further, they are not dependent on the dielectric constant and so a small error is introduced into our value of the enthalpy, see eq 82 in Tomasi et al.[40] The electrostatic correction is strongly dependent on the enthalpy and was included. Thus, the complete function form for the enthalpy is:

$$H = E^0_{gas} + PV + G_{scrf} - T\left(\frac{\partial G_{scrf}}{\partial T}\right)_P \tag{3c}$$

As in the free energy there is a "thermal correction to the enthalpy"; this is analogously composed of the second term of eq 3c and the second two terms of eq 2b.

Results

Gas Phase Geometries and Electronic Structures of $Pb(H_2O)_{1-9}^{2+}$. Initial geometry optimizations of Pb(II)-water clusters using B3LYP with the lanl2DZ(dp) on Pb were unable to find stable gas-phase geometries for a primary

(34) Mennucci, B.; Tomasi, J. *J. Chem. Phys.* **1997**, 5151.
(35) Mennucci, B.; Cancès, E.; Tomasi, J. *J. Phys. Chem. B* **1997**, *101*, 10506.
(36) Reed, A. E.; Weinstock, R. B.; Weinhold, F. *J. Chem. Phys.* **1985**, *83* (2), 735–746.
(37) Maseras, F.; Morokuma, K. *Chem. Phys. Lett.* **1992**, *195* (5−6), 500–504.
(38) Gutowski, K. E.; Dixon, D. A. *J. Phys. Chem. A* **2006**, *110*, 8840–8856.
(39) Floris, F. M.; Selmi, M.; Tani, A.; Tomasi, J. *J. Chem. Phys.* **1997**, *107* (16), 6353–6365.
(40) Tomasi, J.; Mennucci, B.; Cammi, R. *Chem. Rev.* **2005**, *105*, 2999–3093.

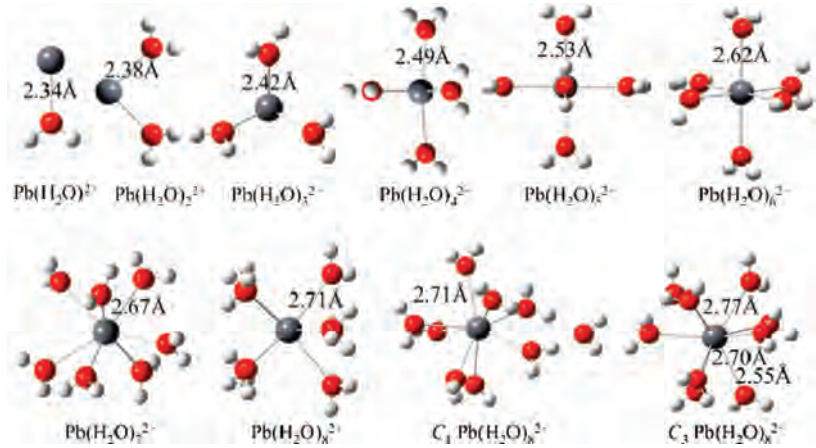

Figure 2. Structural parameters of B3LYP optimized $Pb(H_2O)_{1-9}^{2+}$, average Pb−O bond lengths given in Å (see Supporting Information for complete Cartesian coordinates).

hydration CN greater than 5. While the lanl2DZ $Pb(H_2O)_{1-3}^{2+}$ geometries are similar to those shown in Figure 2 using the aug-cc-pvdz-PP basis on Pb, the tetraquao species exhibited significant bending of the axial Pb−O−Pb angles such that the structure was hemi-directed. Similar hemidirected character was observed in $Pb(H_2O)_5^{2+}$. Attempted optimization of $Pb(H_2O)_6^{2+}$ using the lanl2DZ basis resulted in $Pb(H_2O)_3^{2+}$ with dissociation of the remaining three water ligands. The inability of the lanl2DZ basis to predict stable structures for CN = 6−9 prompted the use of the aug-cc-pvdz-PP basis on Pb, which uses only a small-core 60 e- ECP and describes the $5s^25p^66s^25d^{10}6p^2$ electrons with explicit basis functions (see Computational Methods).

Using the small-core RECP and basis on the aqua-Pb complexes reveals distinct trends in the geometries from coordination numbers 1−9 (Figure 2). In all cases water remains a planar ligand, though hydrogen bonding with increasing coordination number does cause the ligating waters to rotate relative to one another. In the monoaqua species, all atoms are planar. Addition of water to form $Pb(H_2O)_2^{2+}$ results in a 90° O−Pb−O bond angle. Each subsequent addition maintains this angle until the octahedral structure $Pb(H_2O)_6^{2+}$. The seven-coordinate geometry is intermediate and irregular in comparison to the other structures and resembles a monocapped trigonal bipyramid. Octaaqua Pb^{2+} forms a classic square antiprism geometry. The Pb−O bond lengths increase incrementally, by ∼ 0.05Å, with each additional water ligand from CN =1 to 8. Geometry optimization of the nonaaqua species under no symmetry constraints yields a primary hydration shell with CN = 8 in a square antiprism and a ninth water doubly hydrogen bonded in the second hydration shell. Optimization under C_3 symmetry yields a truly nonaaqua species with a distorted tricapped trigonal bipyramidal geometry. The three waters on one side are consistently 0.2 Å shorter than the other side: 2.56, 2.70, and 2.75 Å, respectively, for the three symmetry unique Pb−O bonds. As expected, the C_3 structure had 5 negative frequencies in the range of −50 to −11 cm^{-1}. Thus, in contrast to the structures using the lanl2DZ basis, the aug-cc-pvdz-PP basis on Pb finds even distributed ligand configurations, reminiscent of holo-directed structures, and it further predicts stable hydration geometries with CN = 6−8. In light of the inability to find a low-energy structure with CN = 9 using the small-core ECP and large aug-cc-pvdz-PP basis, geometry optimizations of CN > 9 were not attempted. It should be noted that organo-aqueous Pb(II) species with CN as high as 10 have been observed; however, most of these species are stabilized by a ligand scaffold that prevents the dynamic associative/dissociative processes that would be observed in the purely aqueous species.[41]

While NBO calculations performed on the water clusters indicate that the Pb−O bonds are not covalent, the geometries shown in Figure 2 indicate directed bonding that results from oxygen lone-pair donation into the vacant Pb(II) orbitals. This is in agreement with the Pb(II) atomic charge, q_{Pb} (as calculated by NPA), as a function of increasing hydration number, which decreases by ∼ 0.1−0.05 $e-$ with each additional water: $q_{Pb}^{Pb(H_2O)_1} = 2.000$, $q_{Pb}^{Pb(H_2O)_2} = 1.919$, $q_{Pb}^{Pb(H_2O)_3} = 1.834$, $q_{Pb}^{Pb(H_2O)_4} = 1.751$, $q_{Pb}^{Pb(H_2O)_5} = 1.695$, $q_{Pb}^{Pb(H_2O)_6} = 1.626$, $q_{Pb}^{Pb(H_2O)_7} = 1.578$, $q_{Pb}^{Pb(H_2O)_8} = 1.409$, $q_{Pb}^{C_1Pb(H_2O)_9} = 1.413$, and $q_{Pb}^{C_3Pb(H_2O)_9} = 1.395$.

Based purely upon the structural results, the 90° angle observed between the ligating waters in $Pb(H_2O)_{1-3}^{2+}$ are indicative of oxygen lone-pair donation into non-hybridized 6p-AOs on the Pb. The 5d-AOs are required for the remaining waters to coordinatively bind. This means that the overall sequence of lone-pair donation in coordination numbers 1−8, based upon the structural data, is $6p^1$, $6p^2$, $6p^3$, $6p^35d^1$, $6p^35d^2$, $6p^35d^3$, $6p^35d^4$, and $6p^35d^5$. Given the available unoccupied AOs and the 18 e- rule (assuming each water donates a full electron lone pair), there is only room for eight waters before the period 6 electronic shell is filled. Thus, the ninth water would need to donate into the 7s from the next electronic shell. The natural electronic configurations from the NPA indicate that $Pb(H_2O)_{1-8}^2$ complexes do have water lone-pair electron donation into the 6p and 5d NAOs. Neither the NBO nor the structural results indicate that the 6s-NAO hybridizes with the other NAOs in the same electronic shell. This may be attributed to significant energetic splitting between the Pb 6s and 6p NAOs in the presence of the weakly electron donating water ligands.[1] The absence of 6s hybridization thus has a significant secondary

(41) Rogers, R. D.; Bond, A. H.; Roden, D. M. *Inorg. Chem.* **1996**, *35* (24), 6964–6973.

Table I. B3LYP Thermodynamic Data at 298 K for Gas Phase Sequential Water Addition to Pb^{2+} (eq r1)[a]

product cluster	ΔE/kcal/mol	ΔH/kcal/mol	ΔG/kcal/mol	ΔS/cal/mol K
$Pb(H_2O)_1$	−56.6	−57.2	−50.4	−22.9
$Pb(H_2O)_2$	−44.5	−45.1	−37.0	−27.2
$Pb(H_2O)_3$	−36.3	−36.9	−27.2	−32.4
$Pb(H_2O)_4$	−25.7	−26.3	−17.6	−29.2
$Pb(H_2O)_5$	−22.1	−22.7	−14.6	−27.1
$Pb(H_2O)_6$	−18.2	−18.8	−13.4	−18.1
$Pb(H_2O)_7$	−13.3	−13.9	−4.1	−33.0
$Pb(H_2O)_8$	−12.3	−12.9	−2.7	−34.1
$Pb(H_2O)_9$[b]	−11.8[c]	N/A	N/A	N/A
$Pb(H_2O)_8(H_2O)_1$[b]	−16.0	−16.6	−4.9	−39.2

[a] Only ΔE is presented for $Pb(H_2O)_9^{2+}$ as it is not an energetic minimum. [b] These last two reactions share the Pb octa-aqua complex as reactants. [c] This number does not include either the E_{zpc} or the $E_{thermal}$ for reactants or products.

effect on the overall geometry, that is, ligation is directed by the orientiations of the electron accepting Pb natural atomic orbitals.

The lack of 6s hybridization is in contrast to the MP2/lanl2DZ+d studies of $Pb(H_2O)_4^{2+}$ by Shimoni-Livny which predicted a hemi-directed structure with an axial water angle of 220° and a p-character of 6.5% in the lone-pair orbital (using NPA).[13] To test the impact of the basis upon the calculated electronic and geometric structure, B3LYP geometry optimization of $Pb(H_2O)_4^{2+}$ was performed with the lanl2DZ(dp) basis on Pb and the aug-cc-pvdz on H_2O. The smaller basis resulted in a hemi-directed structure with an axial water angle of nearly identical with the MP2 study, and a p-character in the lone-pair orbital of 6.0% (by NPA). Thus, the enhanced polarization of the lone-pair orbital, and its subsequent impact upon the Pb-water cluster geometry, appears to be largely determined by the basis set choice. Most important, is that the bond angle deviations from 180° in the B3LYP aug-cc-pvdz geometries in $Pb(H_2O)_{1-4}^{2+}$ are the result of under-saturation of the hydration sphere, not 6s hybridization, and tend to decrease with increasing coordination number.

Gas Phase Water Addition Reactions. The gas phase optimized energies for sequential water addition indicate increasing energetic stabilization consistent with the structural results. Table I contains the gas phase hydration data for the following reaction:

$$Pb(H_2O)_{n(g)}^{+2} + (H_2O)_{1(g)} \rightarrow Pb(H_2O)_{n+1(g)}^{+2} \qquad (r1)$$

From the combined structural and energetic results, the favored gas-phase hydration coordination is clearly $Pb(H_2O)_8^{2+}$. All of the water additions are highly exothermic with the exception of the ninth water to the primary hydration shell. A transition in the free energies of addition is seen at $n = 6$, wherein water additions for $n = 1-5$ have ΔG more negative than −10 kcal/mol and later additions have a smaller absolute value. The decrease in ΔG past CN = 6 is consistent with data found in the Cambridge Structural Database (as of 2003), wherein Pb(II) complexes with CN ≥ 7 comprise only 27% of the total number of compounds deposited.[1]

Aqueous Phase Water Addition Reactions. Aqueous phase Pb-water clusters with coordination numbers less than six are highly unlikely and are thus not included in the examination of aqueous water addition. To examine such reactions in solution, the affects of bulk water must be taken into account using the PCM which constructs a solute-containing cavity (generated by a series of overlapping spheres) surrounded by the dielectric field of the solvent. The solvent's polarization interacts with the charge distribution of the solute, resulting in a stabilization energy associated with solvation. Further, the appropriate form of the water reactant must be considered. In direct analogy to the gas-phase reactions, one could use a single water molecule immersed in a PCM cavity; however, this is likely a poor representation of the liquid water from which the reactant molecule is migrating. To examine water addition to Pb(II), we tested two different approaches to determine the "best" representation of a single liquid water molecule. Both approaches use clusters as representations of $H_2O_{(l)}$ immersed in a PCM cavity. In the first approach, the addition of H_2O to $Pb(H_2O)_{5-9}$ is considered wherein the water reactant is leaving a $(H_2O)_{n+1}$ cluster resulting in a $(H_2O)_n$ product. This approach subsequently will be called the "self-consistent" model:

$$Pb(H_2O)_{n(aq)}^{+2} + (H_2O)_{n+1(aq)} \rightarrow Pb(H_2O)_{n+1(aq)}^{+2} + (H_2O)_{n(aq)} \qquad (r2)$$

The second approach for representing liquid water assumes that one liquid water molecule is an average of all the waters in the $(H_2O)_m$ size cluster. This will be called the "averaged" model:

$$Pb(H_2O)_{n(aq)}^{+2} + (1/m)(H_2O)_{m(aq)} \rightarrow Pb(H_2O)_{n+1(aq)}^{+2} \qquad (r3)$$

wherein clusters of $m = 1$, 5, and 9 waters has been examined. The "averaged" model should minimize errors associated with the DFT-PCM geometries of the clusters. In both models, the question of cluster size as a measure of the quality of the representation of liquid water is fundamental to the accuracy of these calculations. Finally, three different PCM cavities (UA0, UFF, and Pauling ($\alpha = 1.1$)) were examined to determine the affect of the bulk water representation on the energetics of water addition (Table II).

In the case of reaction r2 (Table II), wherein the water reactant is leaving a $(H_2O)_{n+1}$ cluster resulting in a $(H_2O)_n$ product, the three PCMs predict that the formation of $Pb(H_2O)_7^{2+}$ is essentially thermally neutral. Formation of the eight-coordinate species is slightly exergonic using the UA0 cavity ($\Delta G = -1.7$ kcal/mol), mildly endergonic using UFF ($\Delta G = 1.2$ kcal/mol), and quite endergonic using the Pauling cavity ($\Delta G = 6.6$ kcal/mol). Water addition to form the C_3 nonaaqua Pb(II) is highly unfavorable by all PCM methods using reaction r2.

Studying the thermodynamic properties of reaction r3 (Table II) reveals a strong dependence of the energies as a function of cluster size and PCM used. In general, the use of the smallest water cluster (H_2O in PCM) yields much more exothermic enthalpies of reaction for water addition than those reactions that utilize $(H_2O)_5$ or $(H_2O)_9$. Deviations in the free energy values using the single (H_2O) cluster may

Table II. B3LYP Thermodynamic Data at 298 K for Solvent Corrected Sequential Water Addition to Form $Pb(H_2O)_n^{2+}$ ($n = 7-9$) Using PCM and the UA0, UFF, and Pauling ($\alpha = 1.1$) Cavities[a]

	$Pb(H_2O)_7$	$Pb(H_2O)_8$	$Pb(H_2O)_9$
	UA0		
ΔH-r2	0.4	1.2	
ΔG-r2	0.0	−1.7	
ΔH-r3 $m = 1$	−6.5	−2.5	
ΔG-r3 $m = 1$	−1.2	3.1	
ΔH-r3 $m = 5$	−4.4	−0.4	
ΔG-r3 $m = 5$	−2.2	2.1	
ΔH-r3 $m = 9$	−4.2	−0.2	
ΔG-r3 $m = 9$	−3.5	0.8	
ΔE-r2			5.2
ΔE-r3 $m = 1$			−0.2
ΔE-r3 $m = 5$			2.8
ΔE-r3 $m = 9$			3.2
ΔE-r4			4.4
	UFF		
ΔH-r2	1.1	4.2	
ΔG-r2	0.8	1.2	
ΔH-r3 $m = 1$	−4.0	−2.0	
ΔG-r3 $m = 1$	−5.4	−4.2	
ΔH-r3 $m = 5$	−2.1	−0.9	
ΔG-r3 $m = 5$	0.2	1.6	
ΔH-r3 $m = 9$	−1.3	−0.1	
ΔG-r3 $m = 9$	−0.6	0.9	
ΔE-r2			4.0
ΔE-r3 $m = 1$			−2.3
ΔE-r3 $m = 5$			1.8
ΔE-r3 $m = 9$			2.7
ΔE-r4			5.5
	Pauling $\alpha = 1.1$		
ΔH-r2	1.3	9.7	
ΔG-r2	1.1	6.6	
ΔH-r3 $m = 1$	−3.7	6.9	
ΔG-r3 $m = 1$	2.0	12.5	
ΔH-r3 $m = 5$	−2.3	8.3	
ΔG-r3 $m = 5$	0.1	10.7	
ΔH-r3 $m = 9$	−2.3	8.3	
ΔG-r3 $m = 9$	−1.5	9.1	
ΔE-r2			4.3
ΔE-r3 $m = 1$			−0.5
ΔE-r3 $m = 5$			2.4
ΔE-r3 $m = 9$			2.9
ΔE-r4			5.0

[a] For $Pb(H_2O)_9^{2+}$ only ΔE values are presented as it is not an energetic minimum.

be attributed to the inability to approximate changes in the entropy difference of water addition, shown subsequently. As in reaction r2, the Pauling cavity yields the least favorable reaction energies for water addition relative to the UA0 and UFF models, which have similar values. As the water cluster size increases (using $(H_2O)_5$ or $(H_2O)_9$), the thermodynamics of water addition begin to resemble that observed in reaction r2, the "self-consistent" approach. Namely, the addition of water to form the seven coordinate species is slightly exergonic, while formation of the octaaquo species is essentially thermoneutral (within computational error, see Table II), and the reaction to form the C_3 nonaaqua species is highly unfavored.

For, the specific case of water addition to CN = 8 to form CN = 9, we also compare the isomerization reaction of a $Pb(H_2O)_8(H_2O)_{1(aq)}^{+2}$ complex (which has a single water in the second hydration shell) to the nonaaqua species:

$$Pb(H_2O)_8(H_2O)_{1(aq)}^{+2} \rightarrow Pb(H_2O)_{9(aq)}^{+2} \quad \text{(r4)}$$

As in reactions r2 and r3, the formation of the nonaaqua species is highly unfavorable by all PCM cavities. Thus the calculations suggest, in light of the rapid water exchange rate for Pb, there is a low probability of the CN = 9 structure in solution. Unfortunately, no experimental data on the geometries of $Pb(II)_{(aq)}$ exist, and only tentative coordination numbers exist that are based upon NMR line broadening in solution, prompting us to benchmark both the computational methods and solvation models against known experimental quantities like the Pb(II) free energy and enthalpy of hydration. These data, shown subsequently, indicate that all $Pb(H_2O)_{6-8}$ species are all thermally accessible at STP and may be present in solution.

Benchmarking Pb Hydration Thermochemistry. ΔG_{hydr} of Pb(II). As previously indicated, to our knowledge the only thermochemical data available for aqueous Pb(II) is the hydration free energy, $\Delta G_{hyd} = -340.6$ kcal/mol, and the hydration enthalpy, $\Delta H_{hydr} = -375.7$ kcal/mol, as derived by Marcus based upon the NBS tables of chemical thermodynamic properties.[11] The error associated with the hydration enthalpy is ∼ 5 kcal/mol, while the error associated with the hydration free energy is not reported. Our goal here is to benchmark the results from varying the PCM cavities and water cluster models against these experimental data. As in the single water addition study, two types of reactions were used to predict Pb(II) hydration (Table III). These represent the "self-consistent" (r5) and the "averaged" approaches (r6) described above:

$$Pb^{+2}_{(g)} + (H_2O)_{n(aq)} \rightarrow Pb(H_2O)_{n(aq)}^{+2} \quad \text{(r5)}$$

and

$$Pb^{+2}_{(g)} + (n/m)(H_2O)_{m(aq)} \rightarrow Pb(H_2O)_{n(aq)}^{+2} \quad \text{(r6)}$$

For reaction r6, clusters of 1, 5, and 9 waters were used and compared against the "self-consistent" reaction r5. As in the single water addition reactions, the thermodynamic values are highly dependent upon the PCM cavity used and the water cluster model employed. Assuming that the experimental values for Pb(II) hydration thermodynamics derive from formation of either of the $Pb(H_2O)_{6-8}^{2+}$ species, and that the nonaaqua species is not present in solution (as indicated by our water addition studies), the UA0 radii generally overestimate hydration free energies by ∼10 kcal/mol, UFF underestimates them by ∼20 kcal/mol, and Pauling cavities underestimate the values by ∼10 kcal/mol. Further, we also observe that the deviations in the results from reactions r5 and r6 diminish with increasing cluster size, consistent with the reactions of water addition.

Using the "self-consistent" approach (reaction r5) with either the UA0 or UFF cavities yields nearly identical ΔG_{hydr} values for the formation of $Pb(H_2O)_{6-8}^{2+}$, while significantly lower ΔG_{hydr} values are predicted for the formation of the nonaaqua species. In the case of the Pauling cavity, the sexa- and septaaqua species have similar free energies of hydration while the octa- and nonaaqua species have significantly lower values. Given the results from the water

Table III. B3LYP PCM Enthalpies (ΔH_{hydr}) and Free Energies (ΔG_{hydr}) of Hydration for $Pb(H_2O)_{6-8}^{2+}$ at 298 K Using Reactions r5 and r6[a]

	r5		r6 ($m = 1$)		r6 ($m = 5$)		r6 ($m = 9$)	
PCM/cluster	ΔH	ΔG	ΔH	ΔG	ΔH	ΔG	ΔH	ΔG
				UA0				
$Pb(H_2O)_6$ ($n = 6$)	−351.0	−349.8	−399.2	−333.9	−344.7	−339.7	−343.3	−347.6
$Pb(H_2O)_7$ ($n = 7$)	−350.6	−349.7	−405.7	−335.1	−349.2	−341.9	−347.6	−351.1
$Pb(H_2O)_8$ ($n = 8$)	−349.4	−351.4	−408.2	−332.0	−349.6	−339.7	−347.8	−350.3
$Pb(H_2O)_8$ $(H_2O)_1$($n = 9$)	−348.7	−348.8	−411.5	−328.2	−350.8	−336.9	−348.7	−348.8
				UFF				
$Pb(H_2O)_6$ ($n = 6$)	−325.1	−324.3	−342.8	−319.5	−323.0	−318.3	−318.1	−322.8
$Pb(H_2O)_7$ ($n = 7$)	−324.0	−323.6	−348.1	−319.5	−325.1	−318.1	−319.4	−323.4
$Pb(H_2O)_8$ ($n = 8$)	−319.9	−322.4	−352.3	−318.1	−326.0	−316.5	−319.5	−322.5
$Pb(H_2O)_8$ $(H_2O)_1$($n = 9$)	−322.0	−322.5	−359.0	−317.5	−329.4	−315.8	−322.0	−322.5
				Pauling				
$Pb(H_2O)_6$ ($n = 6$)	−342.7	−341.6	−342.7	−341.6	−336.7	−331.7	−336.9	−341.2
$Pb(H_2O)_7$ ($n = 7$)	−341.4	−340.5	−341.4	−340.5	−339.0	−331.6	−339.2	−342.7
$Pb(H_2O)_8$ ($n = 8$)	−331.7	−334.0	−331.7	−334.0	−330.7	−321.0	−330.9	−333.6
$Pb(H_2O)_8$ $(H_2O)_1$($n = 9$)	−333.6	−333.8	−333.6	−333.8	−333.4	−319.6	−333.6	−333.8

[a] Experimental: $\Delta G_{hyd}(Pb^{2+}) = -340.6$ kcal/mol, $\Delta H_{hyd}(Pb^{2+}) = -375.7$ kcal/mol.[3,5]

addition reactions, which indicated near isothermal energetics in the formation of the CN = 7 and CN = 8 species, the large deviation in the Pauling ΔG_{hydr} is spurious and indicative of perhaps the poor performance of the Pauling cavities. Prior work in our group has also shown that Pauling radii can lead to poor hydration thermodynamic data for Ln(III) ions.[29]

In the "averaged" model (reaction r6) clear deviations in the calculated ΔG_{hydr} value is observed as a function of the size of the water cluster employed. This is in contrast to the results found in the water addition reactions, wherein very similar results were observed when using $(H_2O)_5$ and $(H_2O)_9$. When the UA0 cavity is used, the free energy of hydration sequentially decreases from −333.9 kcal/mol when using a single water cluster, to −339.7 kcal/mol when using the averaged energy of a water molecule in $(H_2O)_5$, and to −347.6 kcal/mol when employing the energy of water form $(H_2O)_9$. In contrast, the UFF cavity results are all quite similar regardless of the size of the reactant water cluster utilized. Finally, in the case of the Pauling cavity, nearly identical results are found when studying reaction r6 with a single water molecule as when using the averaged energy of a water from $(H_2O)_9$, while the calculated free energy when using $(H_2O)_5$ is nearly 10 kcal/mol more positive. Most important is that in the "self-consistent" approach, the predicted ΔG_{hydr} for $Pb(H_2O)_{6-8}^{2+}$ products lie within 3 kcal/mol using the UA0 and UFF cavities.

To further determine the nature of the deviations in the thermodynamic results for Pb(II) as a function of the PCM cavity, we examined the impact of the calculated Pb(II) atomic charge, q_{Pb}, upon the electrostatic contribution to the free energy of solvation. Examining q_{Pb} as a function of hydration number for each PCM cavity reveals the expected increase in charge transfer with additional waters of hydration. While the UA0 and UFF charges for Pb are relatively similar, the Pauling charges are significantly more positive and are unphysical at low coordination numbers: for example, the Pauling cavity causes the ligating waters to be electron withdrawing rather than donating at CN = 1, 2. This indicates that the Pauling cavity may prevent the ligating waters from properly attenuating the charge, which can have a large impact upon the electrostatic solvent−cavity interactions.

As in previous studies, these results indicate that potentially the largest source of error in accurately determining the hydration free energy is the choice of cavity.[38,42,43] However, an additional source of error may lie in the thermodynamics of water cluster models employed. Benchmarking of the quality of the water clusters is needed to separate the errors in the Pb(II) ΔG_{hydr} calculation into those associated with the water cluster model reactants and those associated with the $Pb(H_2O)_n^{2+}$ product complexes and the PCM models. To test the quality of the water cluster models as representations of liquid water reactants, the energy of water vaporization was determined for each cluster and compared to experiment.

The optimized water clusters determined in this study are consistent with prior work (Figure 3).[44−46]

As in the case for Pb hydration reactions, two different vaporization reactions were compared. The first is the "self-consistent" approach and the second is the "averaged" approach:

$$(H_2O)_{n(aq)} \rightarrow (H_2O)_{n-1(aq)} + H_2O_{(g)} \quad \text{(r7)}$$

and

$$(1/n)(H_2O)_{n(aq)} \rightarrow H_2O_{(g)} \quad \text{(r8)}$$

where the subscript (aq) designates the use of the PCM. In the first reaction, the energies of vaporization will be a result of differences in the cluster structure as one water molecule is removed. The second method focuses on averaging the differences in individual waters within the cluster. We examine both as a function of the size of the cluster to

(42) Cao, Z. J.; Balasubramanian, K. *J. Chem. Phys.* **2005**, *123* (11), 114309.
(43) Takano, Y.; Houk, K. N. *J. Chem. Theory Comput.* **2005**, *1* (1), 70–77.
(44) Xantheas, S. S.; Apra, E. *J. Chem. Phys.* **2004**, *120*, 823.
(45) Xantheas, S. S. *J. Chem. Phys.* **1994**, *100*, 7523.
(46) Maheshwary, S.; Patel, N.; Sathyamurthy, N.; Kulkarni, A. D.; Gadre, S. R. *J. Phys. Chem. A* **2001**, *105*, 10525–10537.

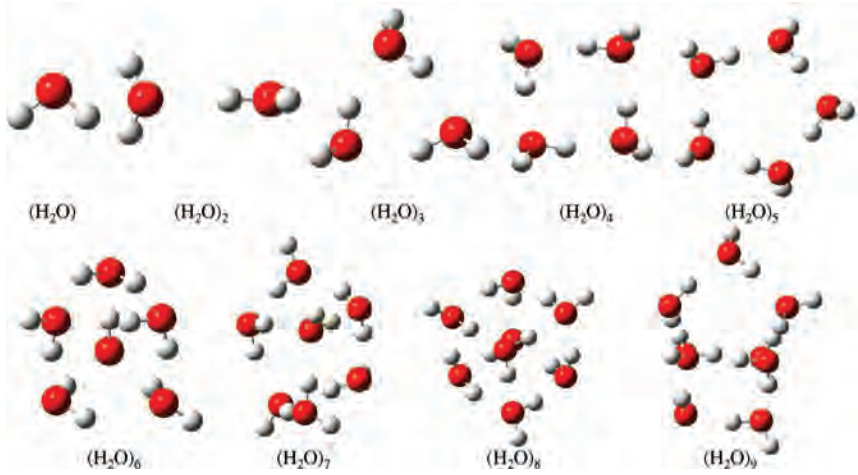

Figure 3. B3LYP/aug-cc-pvdz optimized $(H_2O)_{1-9}$ clusters.

examine different errors that might emerge as a result of the two treatments.

Experimentally, the free energy of water vaporization at 298 K, ΔG_{vap}, is 2 kcal/mol, while the enthalpy $\Delta H_{vap} = 10$ kcal/mol, and the entropy of vaporization $\Delta S_{vap} = 26$ cal/mol K.[47] Figure 4a illustrates the trends in calculated ΔG_{vap} as a function of water cluster size and PCM. Note that the oscillatory behavior exhibited as a function of the water cluster may be attributed to the changes in the cavity size within the PCM (see Supplementary Data) and also entropic effects caused by anharmonicity of the many low frequency vibrational modes present in the cluster. The "averaged" reaction model (reaction r8) exhibits clear convergence trends toward negative ΔG_{vap} values between -0.5 and -2.5 kcal/mol as a function of water cluster size. In general, reaction r7 exhibits significant and extreme oscillatory behavior in the calculated ΔG_{vap} value, mostly likely because of its large dependence upon the accuracy of the water cluster geometry. The UA0 cavity yields the least negative result for the free energy of vaporization (closest to experiment), followed by the Pauling cavity, and finally by the UFF cavity. The experimental enthalpy of vaporization, ΔH_{vap}, is 10 kcal/mol. As seen in Figure 4b, the "averaged" approach (reaction r8) also yields a smooth convergence to chemically reasonable values of ΔH_{vap} at large water cluster sizes, while the "self-consistent" approach exhibits extreme oscillatory behavior similar to Figure 4a. The ΔH_{vap} values span a 3 kcal/mol range as a function of the PCM cavity employed and they are too low relative to experiment by $1-3$ kcal/mol. In the case of the entropy of vaporization, a similar behavior is observed as a function of water cluster size using reactions r7 and r8. The limiting value for ΔS_{vap} using $(H_2O)_9$ is $\sim$30 cal/mol K, which is 4 cal/mol K too high relative to experiment. This is consistent with the deviations in the free energy of vaporization, which is too low by $\sim$4kcal/mol, indicating that the remaining error in the vaporization calculations arises from the inability of the water clusters to properly represent bulk water or potentially the error inherent in our particular combination of method and basis set.

Placed in the context of the benchmarking the Pb(II) hydration thermochemistry, the water vaporization results indicate the following: (1) an error of only $\sim$4 kcal/mol in the Pb(II) hydration thermodynamics may be associated with the model water reactants, and (2) the strong importance of the PCM cavity in affecting Pb(II) hydration thermodynamics occurs at the Pb(II)$-$water cluster product and is not due to large deviations in the PCM energies of the water cluster reactants.

Taking into account the results for single water additions with the absolute hydration results, the best radii overall for evaluating Pb(II) hydration thermodynamics is the UA0. Both the Pauling and the UA0 cavities give free energies of hydration for the 8-coordinate species within 10 kcal/mol of the experimental value, but the UA0 and UFF does better than the Pauling for determining the single water addition energies. As seen in Figure 4, the best DFT thermochemical results had an error of $\sim$4 kcal/mol error. Thus, to assess the most likely coordination numbers of Pb(II) in solution, we use structures within 4 kcal/mol of the lowest energy structure, rather than the traditional $^3/_2kT$ value. This implies that $Pb(H_2O)_{6-8}^{2+}$ are all thermally accessible structural configurations at STP.

ΔH_{hydr} of Pb(II). As seen in Table III, the calculated values of the enthalpy are consistently low by 35 kcal/mol relative to the experimental value once variations due to the choice of cavity in the calculated free energy are considered. When the same method, basis set, and water clusters are used, the vaporization thermodynamics had errors of $\sim$2 kcal/mol for ΔH_{vap} and ΔG_{vap}, and 4 cal/mol K for the vaporization entropy. Given that success in calculating both the free energy and enthalpy of water vaporizaton, it is likely that an important component is missing from the model used in $Pb(H_2O)_n^{2+}$ cluster calculations. The most probably explanation for the "missing" enthalpy component is likely physical: the lack of a second solvation shell. While the second solvation shell has only minimal effect on the total free energy of hydration, there could be a sizable contribution in

(47) CRC handbook of chemistry and physics; http://bibpurl.oclc.org/web/11915; Materials specified: Latest ed. http://bibpurl.oclc.org/web/11915; http://hbcpnetbase.com/ accessed July 20, 2008.

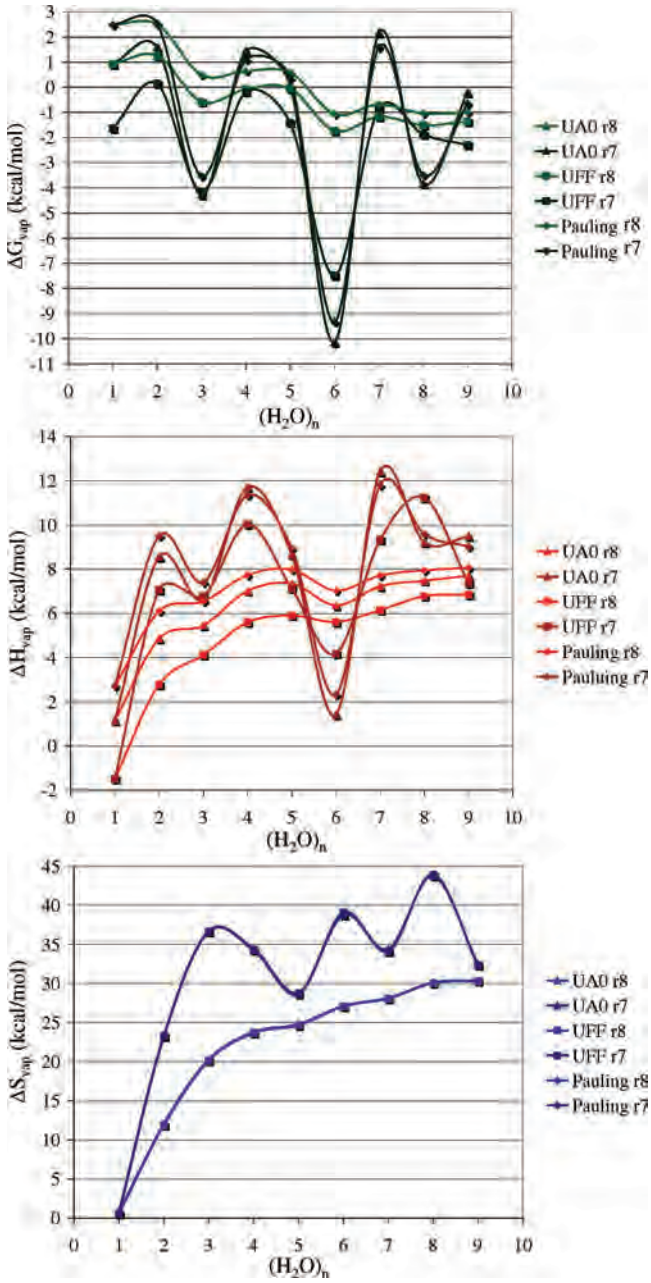

Figure 4. B3LYP/aug-cc-PVDZ thermodynamic parameters of water vaporization as a function of water cluster size (reactions r7 and r8) and PCM cavity (UAO, UFF, Pauling = 1.1).

the form of configurational entropy of the approximately 18 water molecules in that shell, which would significantly alter ΔH_{hydr}. This hypothesis is supported by prior computational studies.[48−53]

(48) Rudolph, W. W.; Fischer, D.; Tomney, M. R.; Pye, C. C. *Phys. Chem. Chem. Phys.* **2004**, *6*, 5145–5155.
(49) Carrillo-Tripp, M.; Saint-Martin, H.; Ortega-Blake, I. *J. Chem. Phys.* **2003**, *118* (15), 7062–7073.
(50) Markham, G. D.; Glusker, J. P.; Bock, C. L.; Trachtman, M.; Bock, C. W. *J. Phys. Chem.* **1996**, *100*, 3488–3497.
(51) Kritayakornupong, C.; Plankensteiner, K.; Rode, B. M. *J. Comput. Chem.* **2004**, *25*, 1576–1583.
(52) Lee, M. A.; Winter, N. W.; Casey, W. H. *J. Phys. Chem.* **1994**, *98*, 8641–8647.
(53) Mejias, J. A.; Lago, S. *J. Chem. Phys.* **2000**, *113* (17), 7306–7316.

Conclusion

The sequential addition of water ligands to Pb(II) has been used as a vehicle to investigate the nature of Pb−OH_2 bonding and to assess the most likely $Pb(H_2O)_n^{2+}$ complexes in aqueous solution. The structural arrangement of water around Pb^{2+} is found to be dominated by vacant 6p and 5d Pb atomic orbitals, which accept small amounts of electron density from the water oxygen lone-pair orbitals. As such, low Pb(II) hydration coordination numbers exhibit what may nominally be called "hemi-directed" structures because of electron-donation into the 6p orbitals; however, these species do not exhibit any polarization of the 6s Pb lone-pair orbital that is typically associated with hemidirected geometries. Further, their geometries exhibit much less hemi-directed character than other Pb(II) complexes with hard ligands. At $Pb(H_2O)_6^{2+}$ more holo-directed structures are observed, which continues until $Pb(H_2O)_8^{2+}$. These geometric and electronic structure results contradict prior theoretical predictions that the hemi- to holo- geometric transition is driven by hybridization changes resulting from enhanced electron donation by the ligands and increased 6p bonding character in the Pb-X bond.[13] No changes in Pb−OH_2 ionic/covalent character is observed as a function of hydration coordination number. We note that prior studies that examined hemi- vs holo-directed ligation in $Pb(H_2O)_4^{2+}$ used a large core 78 e- RECP with a [2s 2p] basis to describe the $6s^2$ electrons. We have shown that this favors the hemi-directed geometry relative to the small core 60 e- RECP with the larger aug-cc-pvdz-PP basis employed in this study. It is further likely that the deviations in geometric and electronic structure as a function of basis set would be observed for other anionic ligand types, and computational studies in this field should be viewed cautiously in the absence of benchmarking data.

The thermodynamic analysis of Pb(II) hydration indicates that $Pb(H_2O)_{6-8}^{2+}$ all reproduce the experimental free energy of hydration for Pb(II) within 10 kcal/mol. Further, the study of sequential water addition reactions indicates that formation of CN 6−8 are all nearly thermoneutral within the errors of the calculation. $Pb(H_2O)_8^{2+}$ represents the maximum coordination number favored in the primary hydration shell. Using our benchmark system of water vaporization, we identify a number of key methodological issues with the correct representation of water as a reactant in the calculation of the thermodynamic values of hydration. Specifically, size consistent approaches should only be used with sufficiently large water clusters since it can actually increase the errors of a calculation when employed with smaller clusters.

Acknowledgment. DOE funding Grant DE-FG07−05ID14692.

Supporting Information Available: A figure and tables containing additional information. This material is available free of charge via the Internet at http://pubs.acs.org.

IC800750G